JCI The Journal of Clinical Investigation

Collective nitric oxide production provides tissue-wide immunity during *Leishmania* infection

Romain Olekhnovitch, … , Andreas J. Müller, Philippe Bousso

Research Article   Microbiology

Nitric oxide (NO) production is critical for the host defense against intracellular pathogens; however, it is unclear whether NO-dependent control of intracellular organisms depends on cell-intrinsic or cell-extrinsic activity of NO. For example, NO production by infected phagocytes may enable these cells to individually control their pathogen burden. Alternatively, the ability of NO to diffuse across cell membranes might be critical for infection control. Here, using a murine ear infection model, we found that, during infection with the intracellular parasite *Leishmania major*, expression of inducible NO synthase does not confer a cell-intrinsic ability to lower parasite content. We demonstrated that the diffusion of NO promotes equally effective parasite killing in NO-producing and bystander cells. Importantly, the collective production of NO by numerous phagocytes was necessary to reach an effective antimicrobial activity. We propose that, in contrast to a cell-autonomous mode of pathogen control, this cooperative mechanism generates an antimicrobial milieu that provides the basis for pathogen containment at the tissue level.

Find the latest version:

https://jci.me/72058/pdf

Collective nitric oxide production provides tissue-wide immunity during *Leishmania* infection

Romain Olekhnovitch,[1,2,3] Bernhard Ryffel,[4] Andreas J. Müller,[1,2] and Philippe Bousso[1,2]

[1]Institut Pasteur, Dynamics of Immune Responses, Paris, France. [2]INSERM U668, Paris, France. [3]Université Paris Diderot,
Sorbonne Paris Cité, Cellule Pasteur, Paris, France. [4]INEM — UMR7355, Molecular Immunology, University of Orléans and CNRS, Orléans, France.
Institute of Infectious Disease and Molecular Medicine, University of Cape Town, Cape Town, South Africa.

Nitric oxide (NO) production is critical for the host defense against intracellular pathogens; however, it is unclear whether NO-dependent control of intracellular organisms depends on cell-intrinsic or cell-extrinsic activity of NO. For example, NO production by infected phagocytes may enable these cells to individually control their pathogen burden. Alternatively, the ability of NO to diffuse across cell membranes might be critical for infection control. Here, using a murine ear infection model, we found that, during infection with the intracellular parasite *Leishmania major*, expression of inducible NO synthase does not confer a cell-intrinsic ability to lower parasite content. We demonstrated that the diffusion of NO promotes equally effective parasite killing in NO-producing and bystander cells. Importantly, the collective production of NO by numerous phagocytes was necessary to reach an effective antimicrobial activity. We propose that, in contrast to a cell-autonomous mode of pathogen control, this cooperative mechanism generates an antimicrobial milieu that provides the basis for pathogen containment at the tissue level.

Introduction

To tackle cell-invasive pathogens, multicellular organisms rely on a wide range of intracellular defense mechanisms. These are induced in infected cells by signals derived from pathogen-associated molecular pattern (PAMPs) recognition and/or by inflammatory cytokines (1). Among these effector mechanisms, the production of nitric oxide (NO) by the inducible NO synthase (iNOS, also known as NOS2) plays a key role against infections by intracellular bacteria (such as *Mycobacterium tuberculosis*, *Listeria monocytogenes*, *Salmonella enterica*) and parasites (*Leishmania* and intracellular *Trypanosoma spp.*) (2). However, how NO production is induced in vivo and results in the control of intracellular pathogens has not been fully clarified.

Cutaneous *Leishmania major* infection in mice is a well-established model to study intracellular defense mechanisms such as NO production. *L. major* parasites reside and replicate in parasitophorous vacuoles (PVs) inside neutrophils and mononuclear phagocytes (mPhagocytes; including macrophages and dendritic cells) (3). Previous studies have demonstrated the central role of NO in the resolution of the infection: iNOS expression in phagocytes results in efficient killing of *L. major* parasites in vitro and is critical for controlling the infection in vivo (4–7).

iNOS induction is a tightly regulated process that requires concomitant activation of the STAT and NF-κB pathways (8). Typically, pioneer in vitro experiments showed that a combination of IFN-γ with LPS or TNF-α efficiently triggered iNOS expression in macrophages (9, 10). Since then, several other stimuli, such as TLR agonists (CpG), costimulatory molecules (CD40L), inflammatory cytokines (Il-1β, IL-17, IL-18), or parasite/bacteria infection, have been shown to be potent iNOS inducers in

vitro (11–15). However, the nature of the signals responsible for iNOS induction in vivo is not fully understood. IFN-γ produced by infiltrating type 1 CD4+ T helper cells (Th1 cells) is known to be critical for iNOS induction (16–18). Several additional signals may be involved, as illustrated by the reduced iNOS expression detected in many knockout animals, such as *Myd88*^{−/−} mice. These signals may act directly on phagocytes to trigger iNOS expression or indirectly, for example, by favoring the development of Th1 cells. Which signal acts in conjunction with IFN-γ to induce iNOS on phagocytes in vivo remains unclear.

Unlike reactive oxygen species, which are directed into the phagosome, NO is synthesized in the cytoplasm of the cell. From there, it can reach PVs and generate toxic compounds, such as peroxynitrite (19), or diffuse outside the cell (20). On the one hand, it has been proposed that efficient pathogen killing required colocalization of iNOS with pathogen-containing compartments (21, 22), suggesting a cell-autonomous control of intracellular pathogens by NO: in this model, individual infected cells would produce effector molecules to control their own pathogen content (1, 23). On the other hand, the fact that NO can diffuse across cell membranes (20) allows for an antimicrobial activity at distance. This could explain how NO acts to control *L. major* parasites in cells that do not appear to express iNOS (7, 24). However, whether the control of intracellular pathogen primarily relies on cell-autonomous NO activity or, on the contrary, requires extensive diffusion between cells has never been experimentally addressed.

Here, we demonstrate that during *L. major* infection, iNOS-expressing cells are incapable of cell-intrinsic control of parasite load. Instead, we provide evidence that the collective production and subsequent diffusion of NO create an antimicrobial milieu that permits parasite killing in cells independently of intrinsic iNOS expression. Altogether, our results identify a cooperative mechanism occurring at the tissue level for the control of intracellular pathogens.
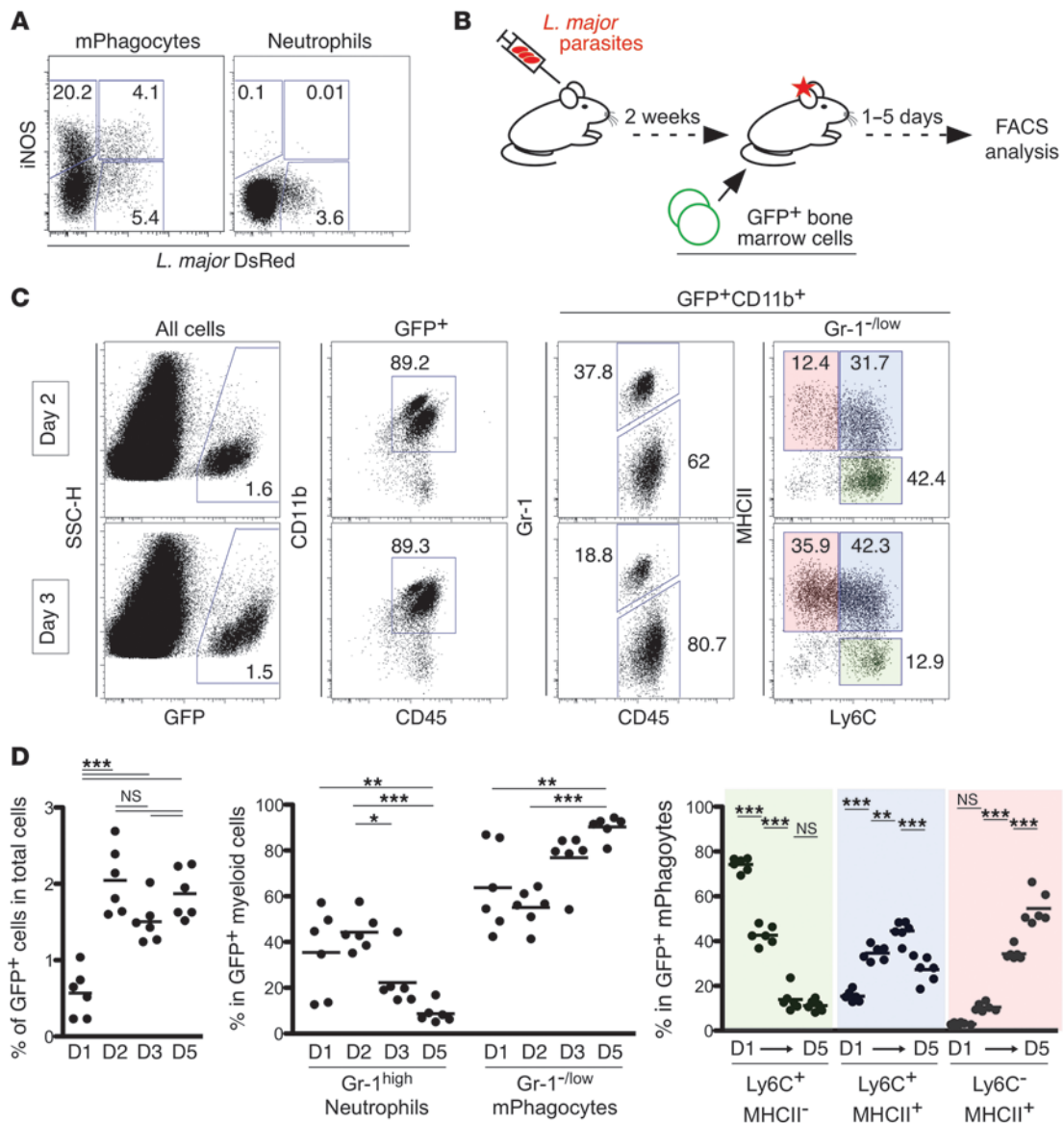
Figure 1
Tracking the fate of recruited phagocytes at the site of infection. (**A**) C57BL/6 mice were infected with DsRed-expressing *L. major* parasites in the ear dermis. Two weeks later, infected ear tissues were stained for intracellular iNOS and analyzed by flow cytometry. (**B**) Experimental set up of BMC transfers. GFP-expressing BMCs were transferred to recipients after 2 weeks of infection. Infected ear tissues were analyzed from day 1 to day 5 after injection by flow cytometry. (**C**) Representative flow cytometry plots of infected ear tissues harvested either 2 or 3 days after BMC injection. (**D**) Plots correspond to cell population frequencies measured by flow cytometry. Green, blue, and pink shading in **C** and **D** identify Ly6C+ MHC class II−, Ly6C+ MHC II+, and Ly6C− MHC II+ cell populations, respectively. Each dot represents an individual ear; horizontal lines represent average values. Numbers shown in flow cytometry profiles represent the percentage of cells falling into the indicated region. *$P < 0.05$; **$P < 0.01$; ***$P < 0.001$. Data are representative of 2 independent experiments.

Results

Recruitment of phagocytes to the site of L. major infection. NO synthesis by the enzyme iNOS is a major effector mechanism against *L. major* infection (20). However, how infection triggers iNOS induction and reciprocally how NO production affects intracellular *L. major* parasites still need to be defined. Using *L. major* parasites expressing a red fluorescent protein (DsRed) (25, 26) and an ear infection model, we observed that both mPhagocytes (Gr-1−/lo MHC II+) and neutrophils (Gr-1hi MHC II−) were infected in the skin tissue, consistent with previous studies (27–29). Substantial iNOS expression was detected

after 2 weeks within mPhagocytes but not in neutrophils (Figure 1A). These mPhagocytes also produced TNF-α, and a substantial fraction expressed CD11c (Supplemental Figure 1; supplemental material available online with this article; doi:10.1172/JCI72058DS1) and were therefore phenotypically similar to the previously described TNF- and iNOS-producing dendritic cell population (30, 31).

Interestingly, most iNOS-expressing mPhagocytes did not contain DsRed fluorescence (Figure 1A and Supplemental Figure 2A). Since DsRed-negative cells did not contain viable parasites (Supplemental Figure 2B), this result suggests that direct
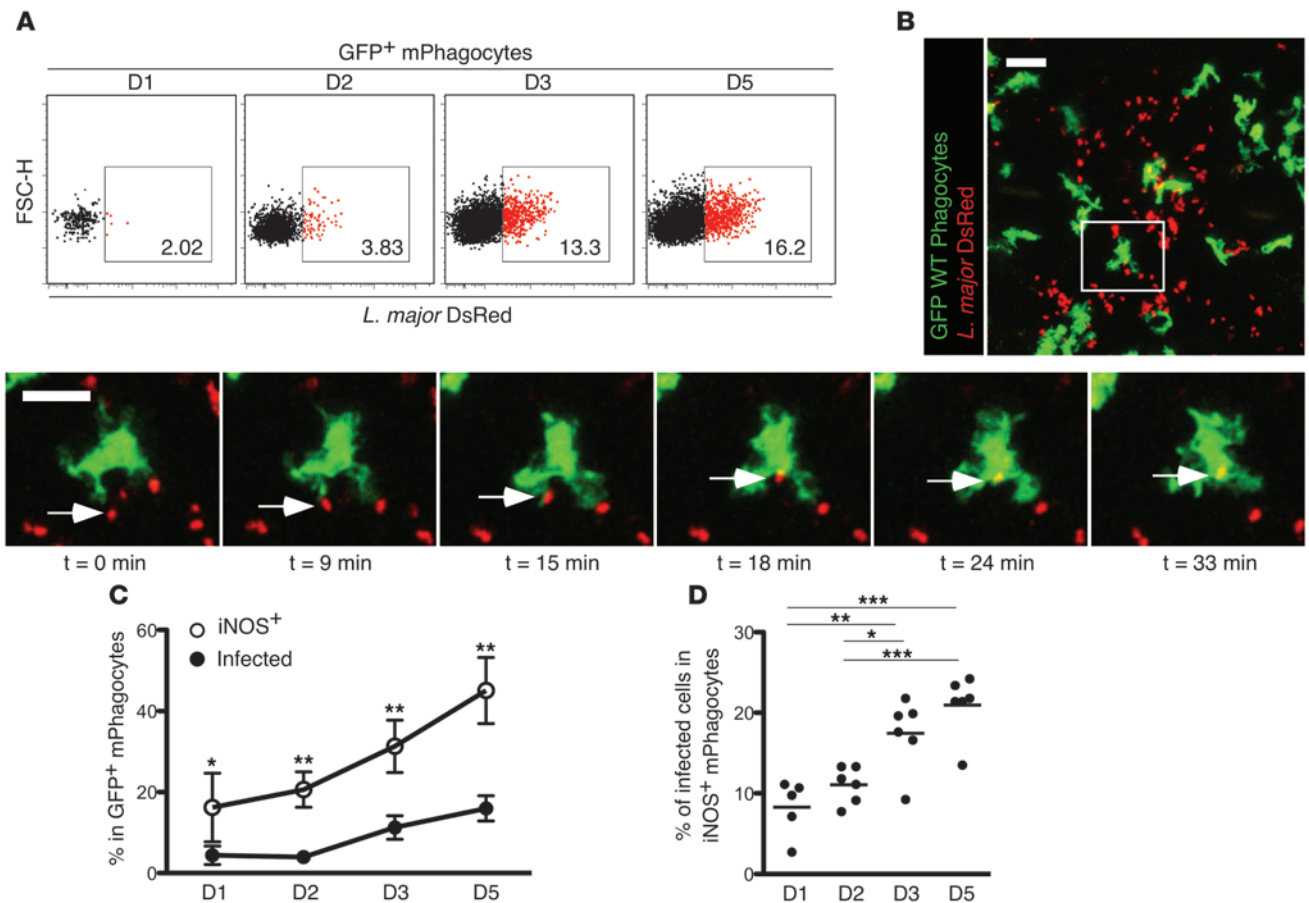
Figure 2
Rapid iNOS induction in mPhagocytes does not require cell infection. C57BL/6 mice were infected with *L. major*, and 2 weeks later, GFP-BMCs isolated from GFP-expressing *Rag2*⁻/⁻ mice were transferred into infected recipients. (**A**) Ear tissues were analyzed from day 1 to day 5 after injection, and infection of GFP-expressing mPhagocytes was followed by flow cytometry. (**B**) Three days after injection, mice were anesthetized and intravital microscopy was performed on infected ears. Time-lapse images show cell invasion by *L. major* parasite. The area delimited by a white rectangle is shown at higher magnification; white arrows indicate the invading parasite. Scale bar: 30 μm (top); 20 μm (bottom). (**C**) Frequency of iNOS-expressing cells and of infected cells within recruited mPhagocytes detected by flow cytometry. (**D**) Frequency of infected cells among iNOS-expressing mPhagocytes from day 1 to day 5 after injection. Horizontal lines represent average values. Numbers shown in flow cytometry profiles represent the percentage of cells falling into the indicated region. *$P < 0.05$; **$P < 0.01$; ***$P < 0.001$. Data are representative of 3 independent experiments.

cell infection is not required for iNOS induction. Alternatively, it is formally possible that these cells were previously infected but have cleared intracellular parasites (hence appearing DsRed⁻).

To distinguish between these possibilities and better define the requirement for iNOS induction, we devised a strategy to follow the response of locally recruited phagocytes in a synchronized manner. To do so, we transferred fluorescent (GFP⁺) bone marrow cells (BMCs) into infected WT recipients and followed recruitment of labeled cells in the infected ear (Figure 1B). Labeled BMCs were efficiently recruited to the site of infection, reaching a plateau on day 2 (Figure 1, C and D). Neutrophils were recruited early on, but their contribution decreased rapidly, accounting for only 10% of fluorescent cells on day 5. The main population of recruited Gr-1⁻/lo cells on day 1 to day 2 was Ly6C⁺ MHC class II⁻ monocytes. At later time points (day 3–5), most recruited cells expressed MHC class II and CD11c and downregulated Ly6C (Figure 1, C and D, and Supplemental Figure 3). Of note, a similar population was observed when purified monocytes (instead of BMCs) were trans-

ferred (Supplemental Figure 4). Our results, together with those of a previous study (32), suggest that monocytes are constantly recruited from the circulation in the infected dermis and differentiate locally into CD11c⁺ MHC class II⁺ cells. Importantly, our strategy provides a mean to track, in a synchronous manner, the fate of recruited monocytes in the infected dermis.

Rapid induction of iNOS does not require cell infection. Since PAMP recognition promotes iNOS induction (13), we next exploited our approach to clarify whether iNOS induction was dependent on cell infection. Upon transfer, a fraction of GFP⁺ phagocytes recently recruited to the site of infection harbored DsRed fluorescence, as detected by flow cytometry (Figure 2A). Using 2-photon imaging of the infected ear, we confirmed that this observation corresponded to actual infection events (Figure 2B and Supplemental Video 1).

Next, we compared these infection rates to the kinetics of iNOS induction in recruited phagocytes. We observed a rapid iNOS induction with 40% of iNOS⁺ cells in recruited phagocytes on day 5 (Figure 2C). Unexpectedly, the percentage of iNOS⁺ cells largely
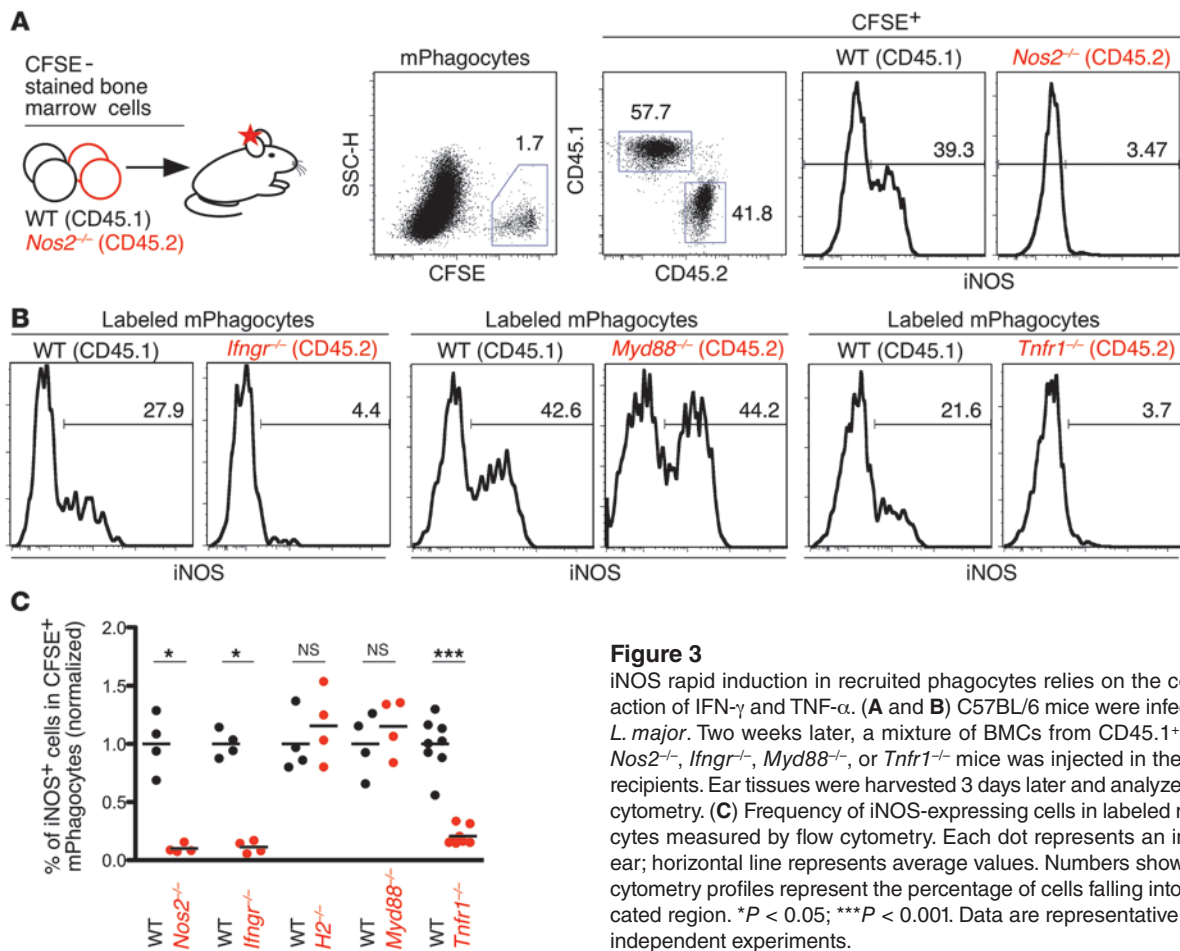
Figure 3
iNOS rapid induction in recruited phagocytes relies on the combined action of IFN-γ and TNF-α. (**A** and **B**) C57BL/6 mice were infected with *L. major*. Two weeks later, a mixture of BMCs from CD45.1+ WT and *Nos2*−/−, *Ifngr*−/−, *Myd88*−/−, or *Tnfr1*−/− mice was injected in the infected recipients. Ear tissues were harvested 3 days later and analyzed by flow cytometry. (**C**) Frequency of iNOS-expressing cells in labeled mPhagocytes measured by flow cytometry. Each dot represents an individual ear; horizontal line represents average values. Numbers shown in flow cytometry profiles represent the percentage of cells falling into the indicated region. *$P < 0.05$; ***$P < 0.001$. Data are representative of 2 to 4 independent experiments.

exceeded that of infected cells (by approximately 4-fold), even at very early time points (Figure 2D). In fact, we could not detect any delay in iNOS induction compared to parasite invasion. Altogether, these results suggest that direct cell infection is not a prerequisite for triggering iNOS expression.

The combined action of IFN-γ and TNF-α is required for iNOS induction in vivo. To delineate the signals responsible for the rapid iNOS induction in recruited mPhagocytes, we injected a mixture of labeled BMCs isolated from specific knockout and congenic CD45.1+ control mice into WT recipients that had been infected 2 weeks before. We then compared iNOS induction in mutant and WT cells recruited in the infected ear 3 days after injection. In these settings and as expected, iNOS staining was detected in WT cells but not in *Nos2*−/− cells (Figure 3).

We have shown previously that CD4+ T cells can induce iNOS in infected cells at distance from their site of antigen recognition, most likely by cytokine diffusion (33). To test whether a similar mechanism operates to induce iNOS in recently recruited cells, we injected a mixture of CD45.1+ WT BMCs with either *Ifngr*−/− or *H2*−/− BMCs. We found that iNOS expression required intrinsic IFN-γR signaling but not MHC class II expression, indicating that direct interaction with CD4+ T cells is not required for iNOS induction in recruited cells (Figure 3C).

It has been shown that efficient iNOS induction requires a combination of two signals, resulting in both STAT and NF-κB activation (8). Although IFN-γ has been clearly identified as one

of these signals (17, 18), the nature of the second signal mediating iNOS induction in vivo during CD4 T cell response has remained elusive. *Myd88*−/− mice show minimal iNOS induction upon infection with *L. major* (27, 34), but it is unclear whether MyD88 signaling is controlling iNOS expression directly at the site of infection or indirectly by promoting T cell priming. Interestingly, in our transfer model, *Myd88*−/− cells were recruited and induced iNOS at similar levels to those of WT cells (Figure 3, B and C). Therefore, MyD88 signaling in mPhagocytes during the effector phase of the immune response is dispensable for iNOS induction in vivo.

An alternative pathway leading to NF-κB activation is TNF-α signaling. In vitro, when combined with IFN-γ, TNF-α efficiently induces iNOS in macrophages (9). However, there are conflicting results concerning its role in vivo (27, 35, 36). With our adoptive transfer system, we could specifically assess the role of TNF-α signaling on mPhagocytes. We found that *Tnfr1*−/− cells were recruited at the site of infection but failed to induce iNOS (Figure 3, B and C). Altogether, our results provide in vivo evidence that the rapid induction of iNOS in recruited mPhagocytes does not require cell infection or MyD88 signaling but instead relies on the combined action of IFN-γ and TNF-α.

iNOS-mediated control of L. major parasite does not operate in a cell-intrinsic manner. Induction of iNOS in phagocytes is known to be the primary intracellular defense mechanism mediating *L. major* parasite control (2, 5–7). Consistently, we found that inhibiting
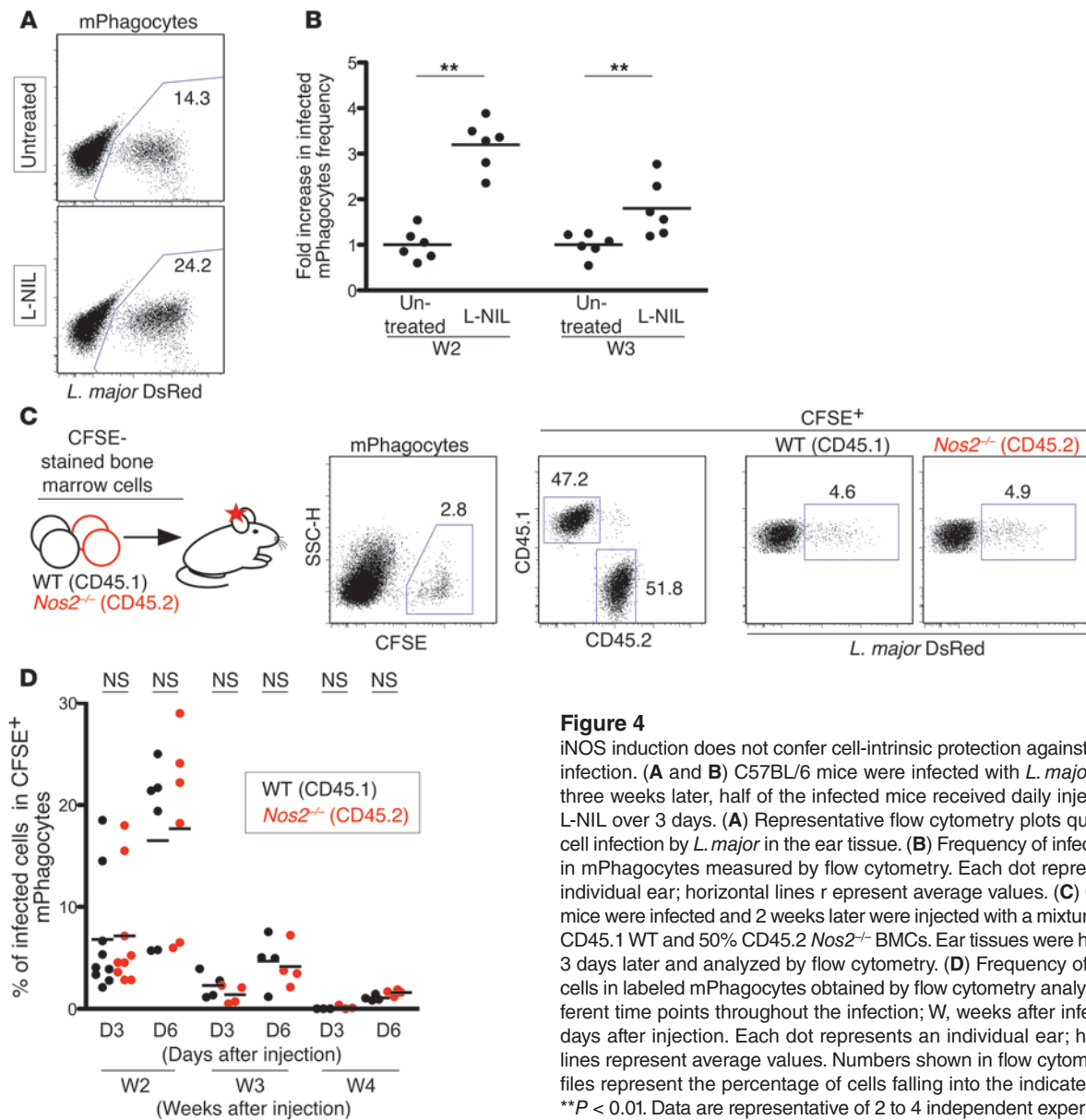
Figure 4
iNOS induction does not confer cell-intrinsic protection against parasite infection. (**A** and **B**) C57BL/6 mice were infected with *L. major*. Two or three weeks later, half of the infected mice received daily injections of L-NIL over 3 days. (**A**) Representative flow cytometry plots quantifying cell infection by *L. major* in the ear tissue. (**B**) Frequency of infected cells in mPhagocytes measured by flow cytometry. Each dot represents an individual ear; horizontal lines r epresent average values. (**C**) C57BL/6 mice were infected and 2 weeks later were injected with a mixture of 50% CD45.1 WT and 50% CD45.2 *Nos2$^{-/-}$* BMCs. Ear tissues were harvested 3 days later and analyzed by flow cytometry. (**D**) Frequency of infected cells in labeled mPhagocytes obtained by flow cytometry analysis at different time points throughout the infection; W, weeks after infection; D, days after injection. Each dot represents an individual ear; horizontal lines represent average values. Numbers shown in flow cytometry profiles represent the percentage of cells falling into the indicated region. **$P < 0.01$. Data are representative of 2 to 4 independent experiments.

iNOS with L-N^6-(1-iminoethyl)lysine dihydrochloride (L-NIL) for as few as 3 days during an ongoing immune response resulted in an increased frequency of infected cells (Figure 4, A and B). Thus, we predicted that the rapid induction of iNOS in recruited phagocytes should allow these cells to efficiently control the parasite. To test this, we injected a mixture of iNOS-deficient (*Nos2$^{-/-}$*) and CD45.1$^+$ WT BMCs into recipient mice that had been infected 2 to 4 weeks earlier and compared infection in the 2 populations of recruited phagocytes at days 3 and 6 after injection (Figure 4C). Overall, the rate of infection in recruited mPhagocytes decreased with the development of the immune response: it ranged from 17% at day 6 after injection into animals infected for 2 weeks to 2% when animals were infected for 4 weeks (Figure 4D). Surprisingly, we found that WT and *Nos2$^{-/-}$* cells recruited to the site of infection were infected with the same efficiency, irrespective of the time point tested. Thus, iNOS-expressing phagocytes did not appear to better control *L. major* parasites

when compared with their nonexpressing counterparts, suggesting that the antileishmanial activity of iNOS does not operate in a cell-intrinsic manner.

iNOS-expressing cells provide pathogen control at the tissue level. In contrast to a cell-autonomous mode of parasite control, we hypothesized that a limited number of iNOS-expressing cells could exert efficient antimicrobial activity in trans and act at the tissue level. To test this model, we generated mixed bone marrow chimeras reconstituted with a 1:1 mixture of *Nos2$^{-/-}$* and CD45.1 WT bone marrow (Figure 5A). Strikingly, *Nos2$^{-/-}$* and WT cells were infected with the same efficiency at all time points tested, despite the fact that 40% of WT infected cells expressed iNOS (Figure 5, B and C, and Supplemental Figure 5). In addition, inhibition of iNOS at week 3 resulted in a similar increase in parasite load in *Nos2$^{-/-}$* and WT phagocytes (Figure 5C), confirming that the control of the infection in both cell compartments depended on NO. These results were consistent with our
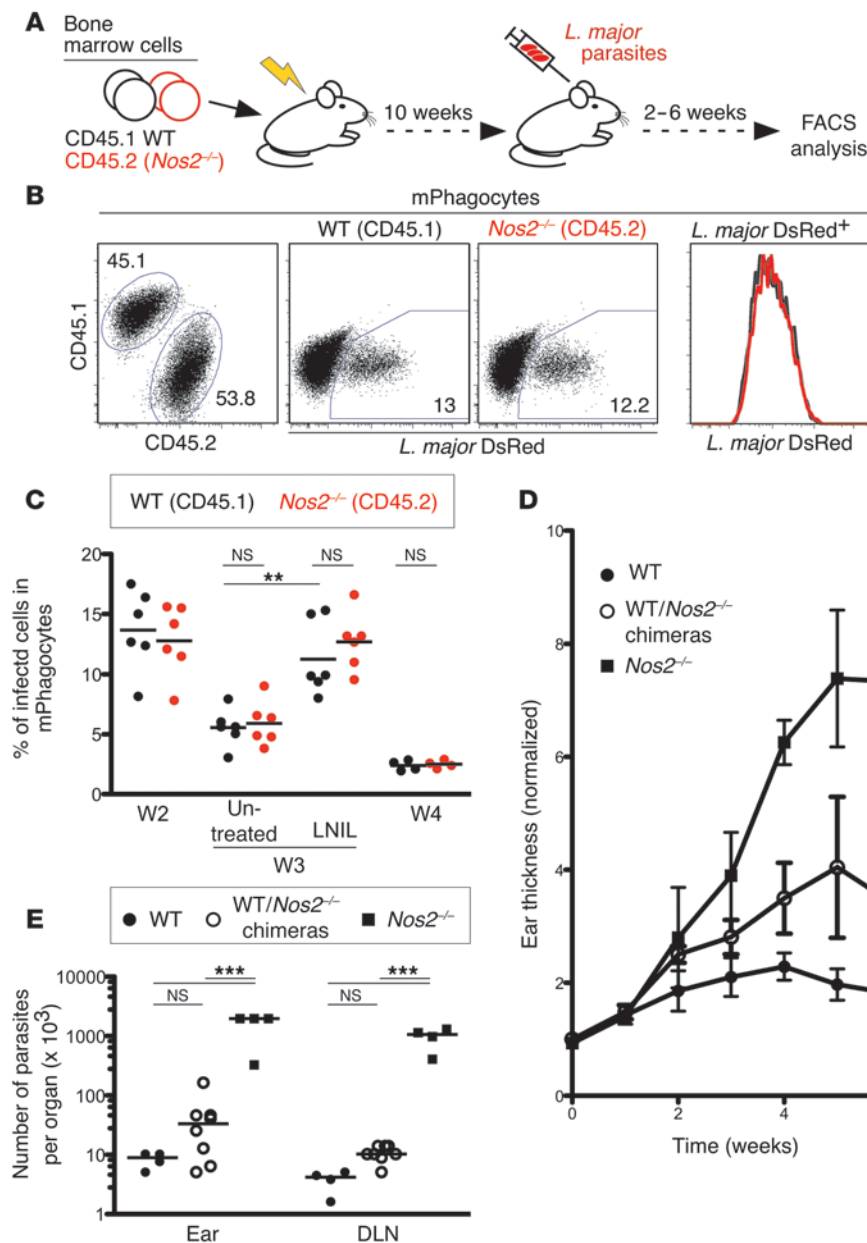
Figure 5
iNOS-expressing cells provide parasite control at the tissue level. (**A**) Lethally irradiated CD45.1 C57BL/6 WT mice were reconstituted with a mixture of 50% CD45.1 WT and 50% CD45.2 *Nos2⁻/⁻* BMCs. Mixed bone marrow chimeras were infected with DsRed-expressing *L. major* parasites in the ear dermis and, 2 to 6 weeks later, infected ear tissues were analyzed by flow cytometry. (**B**) Representative flow cytometry plots of infected ear tissues from mixed bone marrow chimeras. (**C**) Frequency of infected cells among CD45.1 WT and CD45.2 *Nos2⁻/⁻* mPhagocytes in the ear measured by flow cytometry. At week 3, half of the mouse group received daily injection of L-NIL over 3 days (LNIL) or were left untreated. (**D**) Ear thickness of C57BL/6, mixed bone marrow chimeras, and *Nos2⁻/⁻* mice. Plot values represent normalized thickness mean ± SD. (**E**) Parasite counts per infected ear or per draining lymph node (DLN) at week 6 after infection. Each dot represents an individual ear; horizontal lines represent average values. Numbers shown in flow cytometry profiles represent the percentage of cells falling into the indicated region. **$P < 0.01$; ***$P < 0.001$. Data are representative of 2 independent experiments.

transfer experiments and provided additional evidence that the antimicrobial effect of iNOS was not cell intrinsic. Most importantly, we found that mixed bone marrow chimeras efficiently controlled the infection in contrast with *Nos2⁻/⁻* mice (Figure 5, D and E). We conclude that the subset of iNOS-competent cells provides parasite control at the tissue level (including in iNOS-deficient cells), most likely by exerting antimicrobial activity in trans.

Diffusion of nitrogen species allows for parasite control independently of intrinsic iNOS expression. To monitor the relative efficiency of parasite control in trans, we designed an in vitro assay to simultaneously monitor parasite contents in iNOS-competent and -deficient phagocytes. *Nos2⁻/⁻* and WT macrophages were cultured separately or together and infected with *L. major*. After 2 days, macrophages were activated for iNOS induction (Figure 6A). This treatment resulted in a substantial decrease in parasite load in WT but not

in *Nos2⁻/⁻* cells (when cultivated alone). However, the reduction in parasite load within *Nos2⁻/⁻* cells was rescued when these cells were cocultured with iNOS-competent cells (Figure 6B). In fact, parasite control in *Nos2⁻/⁻* cells was indistinguishable from that observed in WT cells (Figure 6, B and C), underlining the high efficiency of iNOS antimicrobial activity in trans.

To test whether the cell-extrinsic effect of iNOS required direct cell contact, we incubated infected *Nos2⁻/⁻* macrophages with activated WT or *Nos2⁻/⁻* cells in Transwell inserts. Interestingly, activated WT macrophages could restore parasite control in *Nos2⁻/⁻* cells, even in a Transwell assay (Figure 6D). Of note, this rescue was slightly delayed in Transwell inserts as compared with that in mixed cultures (requiring an additional day), possibly due to a concentration effect. Nonetheless, our observations revealed a role for a diffusible iNOS product in mediating uniform parasite control in producing and bystander cells.
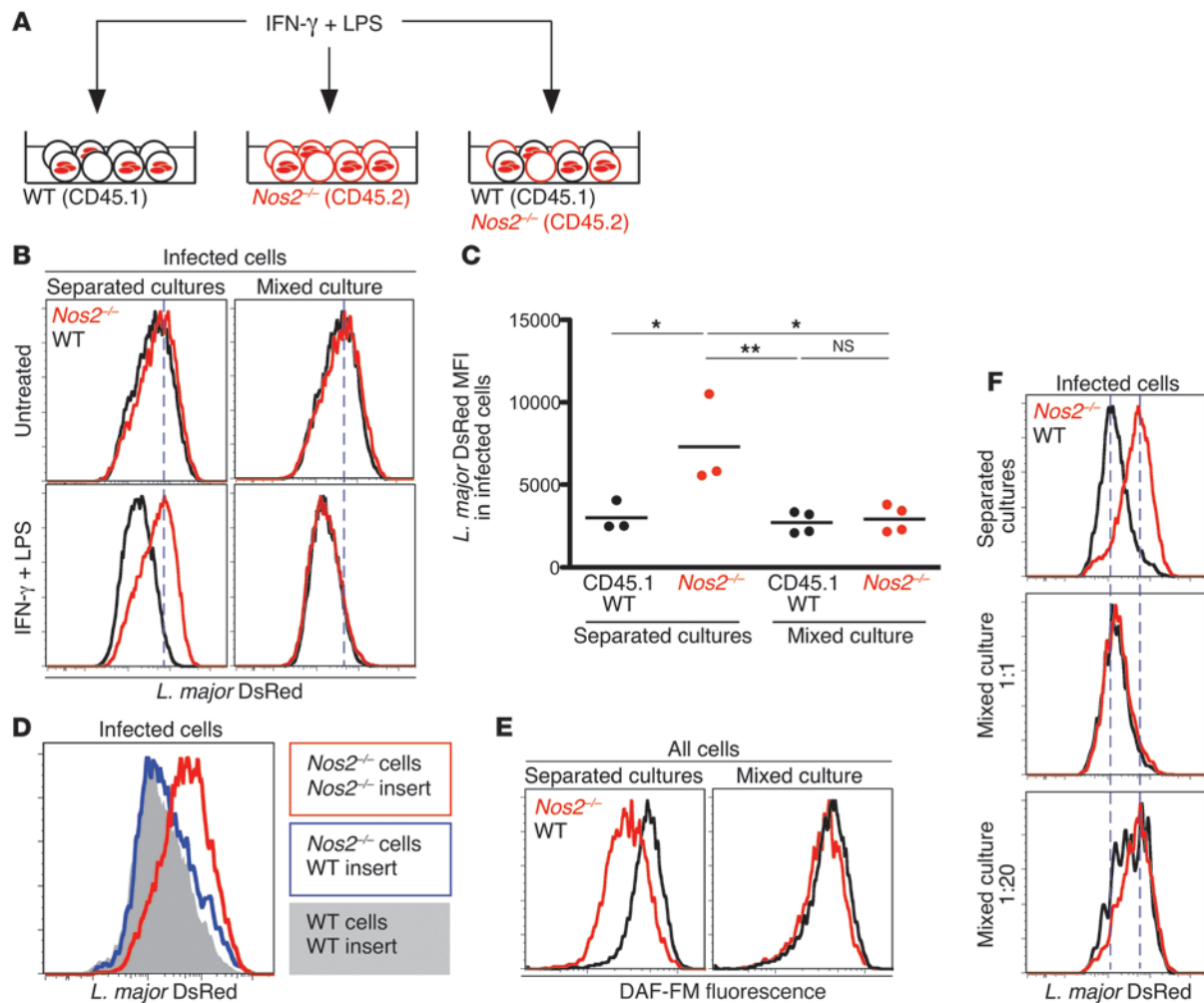
Figure 6
The diffusion of iNOS-derived products allows for parasite control in trans. (**A**) Peritoneal macrophages from CD45.1 WT and CD45.2 *Nos2*–/– mice cultured separately or together were infected with DsRed-expressing *L. major* parasites. Two days later, cells were activated over 48 hours with LPS and IFN-γ or left untreated and analyzed by flow cytometry. (**B**) Representative histograms of DsRed fluorescence in infected cells treated or not with IFN-γ and LPS. Dashed lines mark the peak of *L. major* DsRed fluorescence in untreated *Nos2*–/– cells. (**C**) *L. major* DsRed mean fluorescence intensity in infected cells, as measured by flow cytometry. Each dot represents an individual well; horizontal lines represent average values. (**D**) Histograms of DsRed fluorescence in peritoneal macrophages. *Nos2*–/– macrophages were infected and activated over 72 hours in the presence of either activated *Nos2*–/– (red) or WT (blue) infected macrophages in Transwell inserts. DsRed fluorescence in control WT cells is shown as solid gray. (**E**) Infected CD45.1 WT and CD45.2 *Nos2*–/– peritoneal macrophages were activated separately or in coculture. DAF-FM staining was performed 24 hours after activation and measured by flow cytometry. (**F**) Infected CD45.1 WT and CD45.2 *Nos2*–/– peritoneal macrophages were activated separately or in coculture at different WT/*Nos2*–/– ratios. DsRed fluorescence in infected cells was measured 48 hours later by flow cytometry. Dashed lines mark the peaks of DsRed fluorescence in WT and *Nos2*–/– cells cultured separately. *$P < 0.05$; **$P < 0.01$. Data are representative of 3 independent experiments.

To evaluate the efficiency of NO diffusion, we stained macrophages with DAF-FM, a fluorescent probe for NO (37). Upon activation, WT macrophages displayed elevated DAF-FM fluorescence when compared with that of *Nos2*–/– cells cultivated alone. Importantly, when cocultured with activated WT macrophages, *Nos2*–/– cells exhibited increased DAF-FM fluorescence (Figure 6E), similar to WT levels. Thus, iNOS-derived products diffuse very effectively from iNOS-competent to iNOS-deficient cells.

NO most likely controlled parasite burden at distance by mediating direct toxic activity on the parasite. However, it was formally possible that NO acted indirectly as a signaling molecule on macrophages to upregulate their antimicrobial activity. To distinguish between these

possibilities, we cultured free *L. major* parasites with activated macrophages in a Transwell setting. Consistent with the known susceptibility of *L. major* parasites to NO (38), we found that activated WT macrophages but not *Nos2*–/– macrophages affected the viability of spatially separated free parasites (Supplemental Figure 6). Although this assay was performed with promastigotes (that may differ in sensitivity from the intracellular amastigote form), this result suggested that NO exerted a direct toxicity on parasites. In sum, the effective diffusion of NO resulted in an equivalent antimicrobial activity in all phagocytes, irrespective of their intrinsic iNOS expression.

Parasite killing requires collective NO production. Diffusion of NO could represent a byproduct of iNOS-expressing macrophages
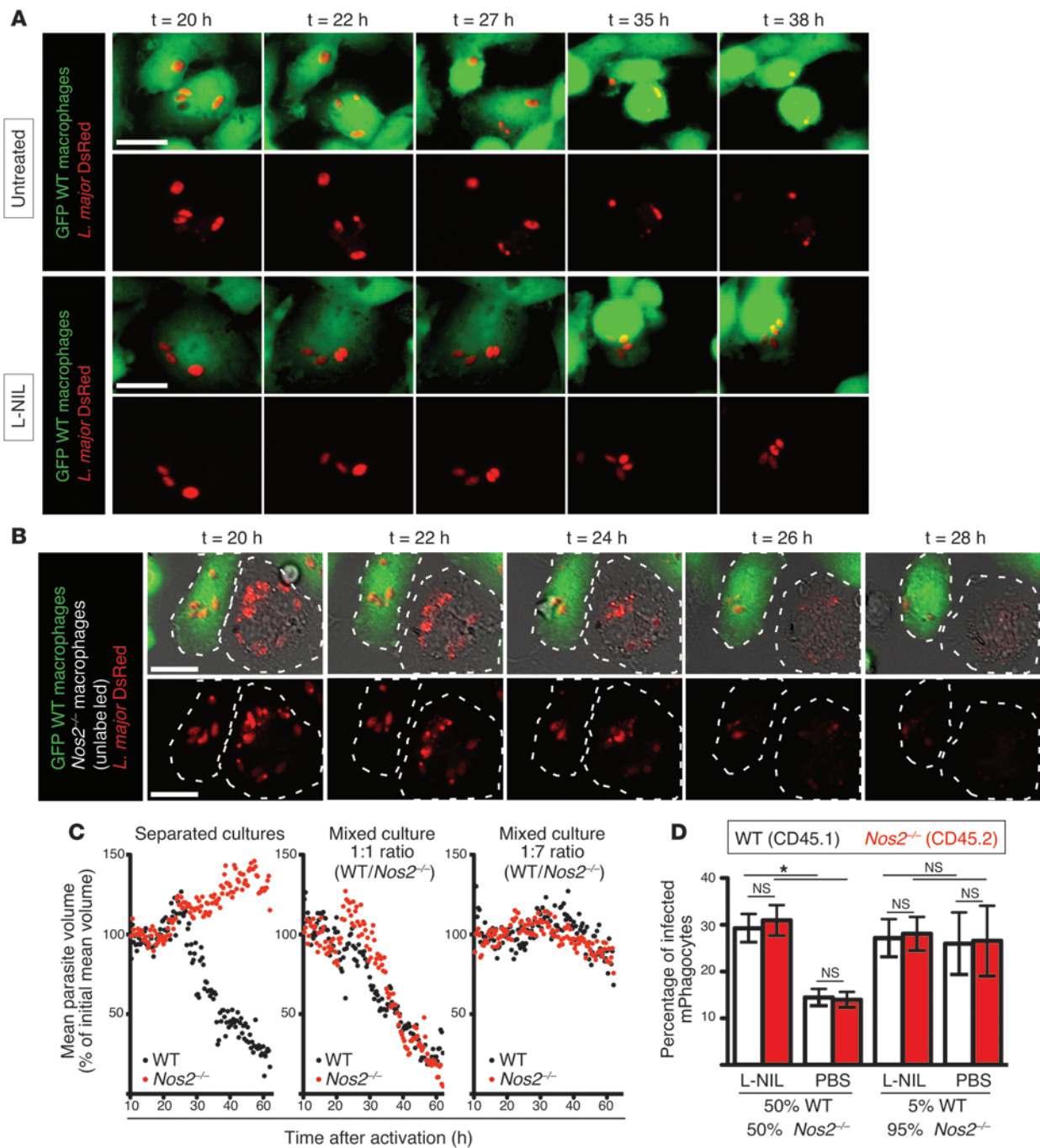
Figure 7

Parasite killing requires collective NO production. (**A**) Infected peritoneal macrophages from GFP-expressing mice were activated in the presence or in absence of L-NIL. Eighteen hours after activation, time-lapse microscopy was performed for up to 48 hours. Scale bar: 20 μm. (**B**) A mixture of infected peritoneal macrophages from WT GFP+ and *Nos2*−/− mice was activated. After 10 hours, time-lapse microscopy was performed for up to 48 hours. Dashed lines indicate the outline of the cells, as identified on bright-field images. Scale bar: 20 μm. (**C**) Mean volume of parasites contained in *Nos2*−/− cells (red dots) or GFP+ WT cells (black dots) over time and in different conditions (separated cultures and mixed cultures with 1:1 and 1:7 WT/*Nos2*−/− ratios). Volume is expressed as a percentage of initial volume. On average, 60 parasites were analyzed at each time point. Data are representative of 2 independent experiments. (**D**) Lethally irradiated CD45.1 C57BL/6 WT mice were reconstituted with a mixture of 50% (or 5%) CD45.1 WT and 50% (or 95%) CD45.2 *Nos2*−/− BMCs. Mixed bone marrow chimeras were infected with DsRed-expressing *L. major* parasites in the ear dermis. Two weeks later, half of infected mice received daily injections of L-NIL over 3 consecutive days. Infected ear tissues were then harvested and analyzed by flow cytometry. The graph shows the frequency of infected cells among CD45.1 WT and CD45.2 *Nos2*−/− mPhagocytes (mean ± SEM). *$P < 0.05$.

that control parasites autonomously. Alternatively, the diffusion of NO from a large number of cells may be required to build up a high enough concentration in the environment that will allow for parasite control. Supporting the latter hypothesis, we found that when we increased the *Nos2*⁻/⁻ to WT cell ratio in culture, the reduction of parasite load was lost in both cell types (Figure 6F). Thus, iNOS-competent cells were no longer capable of parasite control when they were surrounded by a majority of iNOS-deficient cells.

Because the kinetics of *L. major* parasite clearance are very slow, it has been difficult to clarify how NO participates in pathogen control. To characterize the iNOS-mediated effect in trans observed in flow cytometry assays and define its dynamics, we performed time-lapse videomicroscopy on infected macrophages cultures for up to 2 days. Upon activation of *L. major*–infected WT macrophages, intracellular parasites progressively shrunk, lost their normal morphology, and ultimately disappeared (Figure 7A and Supplemental Video 2). This was not the case in L-NIL–treated cells (Figure 7A) or *Nos2*⁻/⁻ cells (Figure 7C and Supplemental Video 3) cultured alone, in which parasites appeared to remain intact. However, parasite killing was restored in *Nos2*⁻/⁻ macrophages when cultured in the presence of iNOS-competent cells (Figure 7B and Supplemental Video 4). Thus, the diffusion of iNOS products occurs in proportions that permit parasite killing in trans. Strikingly, when we compared parasite volumes in *Nos2*⁻/⁻ cells and in WT cells, we could observe that parasite shrinkage occurred simultaneously in both cell types, suggesting that *Nos2*⁻/⁻ cells have a similar access to NO compared with that of WT cells (Figure 7C). Moreover, parasite killing was similarly delayed in both cell types when the proportion of WT cells in culture was reduced. These results strongly suggest that parasite killing in macrophages requires a minimum concentration of NO and that NO is equally available to iNOS-deficient and -competent cells.

To test whether the model is relevant in vivo, we generated mixed bone marrow chimeras containing either a high (50%) or low (5%) frequency of iNOS-competent cells. We noted that both iNOS-competent and *Nos2*⁻/⁻ phagocytes were highly infected in 5% chimeric mice compared with 50% chimeric animals (Figure 7D). To assess whether the low fraction of iNOS-competent cells could nevertheless participate in parasite control, we treated these chimeras with L-NIL. In contrast to what was observed in 50% chimeric mice, L-NIL treatment did not result in increased parasite load in 5% chimeric mice, suggesting that NO production in these mice was insufficient to trigger parasite control, even in iNOS-competent cells (Figure 7D). We obtained similar results using adoptive transfer of iNOS-competent and -deficient cells in infected *Nos2*⁻/⁻ mice (Supplemental Figure 7). These in vivo results further confirmed the poor efficiency of intrinsic iNOS activity and the requirement for a high proportion of iNOS-producing cells for the control of the infection.

Altogether, our results indicate that the diffusion of NO collectively produced by iNOS-expressing cells, is critical for parasite killing, which occurs independently of intrinsic iNOS expression. We propose that this cooperative mechanism enables the host to contain intracellular pathogen at the tissue level.

Discussion

NO has been identified as a major effector molecule against many intracellular pathogens infections (2). However, how NO production is induced in vivo and exerts its antimicrobial properties has remained unclear. While iNOS activity is indispensable for con-

trolling *L. major* infection, we found that the rapid induction of iNOS in mPhagocytes did not confer them any cell-intrinsic ability to control the parasites. Instead, we established that the collective production of NO by mPhagocytes and the subsequent diffusion of reactive nitrogen species were required to reach a concentration high enough to control intracellular pathogens at the tissue level.

We have dissected the signals promoting iNOS expression in vivo. In vitro studies have demonstrated that a combined effect of signals derived from PAMP recognition and IFNs is critical for iNOS induction (10, 39). Consistently, mice deficient for IFN-γ (40, 41) or MyD88 signaling (34) have been previously shown to exhibit a dramatic reduction in iNOS expression upon *L. major* infection. We demonstrated that iNOS was rapidly induced in mPhagocytes that are recruited to the lesion and confirmed the dependence on IFN-γ signaling. In contrast, this induction did not require cell infection by *L. major* parasites and was not affected by MyD88 deficiency in mPhagocytes. Therefore, while MyD88 may be important for T cell activation by antigen-presenting cells (42) or IL-1 signaling (43), it appears to be dispensable in recruited phagocytes for iNOS induction. TNF-α has been shown to be sufficient to induce iNOS in vitro when combined with IFN-γ (9), but its role in vivo, assessed using deficient mice, has yielded conflicting results (27, 36). By assessing the role of TNF-α signaling specifically in phagocytes at the site of *L. major* infection, we showed that iNOS induction in vivo critically depended on TNF-α. While T cells are clearly the major source of IFN-γ, both T cells and mPhagocytes contribute to TNF-α production (16, 44, 45). Thus, soluble factors rather than direct pathogen recognition drive the rapid induction of iNOS at the site of infection, resulting in iNOS expression in numerous mPhagocytes. Consistent with this idea, a recent study highlighted the importance of soluble factors for NO-mediated control of *Leishmania amazonensis* (15). These observations prompted us to investigate how these recruited iNOS-expressing phagocytes contribute to microbial killing in vivo.

NO can diffuse across cell membranes, a process involved in many biological processes (20), such as downregulation of T cell responses (46), inhibition of tumor cell mitochondrial respiration and DNA synthesis (47), and inhibition of viral replication (48). Along this line, it has been suggested that NO produced by macrophages could also contain *L. major* infection in neighboring fibroblasts (7, 24). Whether NO diffusion and activity in trans is the predominant mechanism promoting the control of *L. major* has not been addressed so far. In fact, intracellular control of *Salmonella* in macrophages was shown to require colocalization of iNOS itself with pathogen-containing compartments (21, 22), suggestive of a cell-intrinsic mode of action. On the contrary, we showed that the intrinsic activity of iNOS was negligible both in vitro and in vivo. Interestingly, our in vitro imaging assay revealed efficient killing of intracellular parasites in iNOS-deficient cells with very limited host cell death, suggesting that iNOS products displayed the highest toxicity in PVs, possibly when encountering reactive oxygen species (49) or acidic conditions (38). Such a 2-step mechanism would ensure a compartmentalized toxicity mediated by a diffusible molecule.

Strikingly, we show that the collective action of phagocytes is required to reach a threshold concentration of NO above which the pathogen can be contained efficiently. Notably, this model assigns a critical role for the numerous uninfected phagocytes expressing iNOS at the site of infection. By contributing to the

generation of an antimicrobial milieu, these cells actively participate in the defense against intracellular pathogens. This issue is in fact relevant to many infectious agents, including *L. monocytogenes*, which drives the accumulation of high numbers of uninfected TNF- and iNOS-producing dendritic cells (30). Moreover, as many intracellular pathogens, including *L. major*, set up strategies to limit NO production in infected cells (50, 51), the ability of uninfected cells to produce NO available for neighboring cells could be critical for the control of the infection.

We have shown previously that a small number of antigen presentation events can induce widespread iNOS expression through diffusion of T cell–derived cytokines (29, 33). The present study suggests that this bystander effect is further amplified by the activity of iNOS-expressing cells in trans. This double-layered propagation of effector functions likely provides an effective strategy for the containment of intracellular pathogen in the infected tissue. Of note, we have recently observed that, in the first weeks of infection, NO could limit parasite metabolism without systematically inducing parasite death (52). The lethal and sublethal modes of parasite control mediated by NO likely correspond to distinct concentrations collectively produced by recruited phagocytes.

In sum, our results elucidate the mode of action of iNOS products, whereby the cooperative activity of phagocytes permits pathogen control rather than the triggering of cell-autonomous defense mechanisms. Defining the parameters that optimize the generation of such an antimicrobial milieu should provide new strategies to fight infections by intracellular pathogens.

Methods

Mice. WT C57BL/6 and CD45.1 (B6.SJL-*Ptprc^aPepc^b*/BoyJ) mice were purchased from Charles River Laboratories. MHC class II–deficient (B6.129S2-*H2^dlAb1–Ea*) (53), IFN-γ receptor 1–deficient (B6.129S7-*Ifngr1^tm1Agt*) (54), ubiquitin-GFP [C57BL/6-Tg(UBC-GFP)30Scha] (55), MyD88-deficient (B6.129P2-*Myd88^tm1Aki*) (56), TNFR1-deficient (B6.129P2-*Tnfrsf1a^tm1Blt*) (57), and iNOS-deficient (B6.129P2-*Nos2^tm1Lau/J*) (58) mice were bred under specific pathogen–free conditions at Institut Pasteur. For generating bone marrow chimeras, WT C57BL/6 recipients were γ-irradiated twice within 3 hours with 5.5 Gy and reconstituted with a mixture of 2×10^7 CD45.1 BMCs and 2×10^7 *Nos2^–/–* BMCs intravenously. For chemical inhibition of iNOS in vivo, C57BL/6 mice received daily intravenous injection of 11.5 mg/kg L-NIL (Sigma-Aldrich) in PBS over 3 days (59).

Parasites. DsRed-expressing parasites (25, 26) were grown at 26°C for a maximum of 5 passages in M119 medium supplemented with 10% heat-inactivated fetal bovine serum, 0.1 mM adenine, 1 μg/ml biotin, 5 μg/ml hemin, and 2 μg/ml biopterin (all from Sigma-Aldrich). For infection, 10^5 stationary-phase promastigotes were resuspended in 10 μl PBS and injected into the ear dermis. For long-term infections, ear thickness was measured weekly with a Mitutoyo Caliper Thickness Gauge. Parasite load in each infected ear or draining lymph node was determined by a limited dilution assay. Ears were separated into dorsal and ventral sheets using jagged forceps and digested in RPMI 1640 medium containing 1 mg/ml collagenase and 50 ng/ml DNase (Sigma-Aldrich) for 45 minutes at 37°C and then passed through a 70-μm cell strainer. Tissue homogenates were serially diluted in a 96-well flat-bottom plate containing M119 medium supplemented with 10% heat-inactivated fetal bovine serum, 0.1 mM adenine, 1 μg/ml biotin, 5 μg/ml hemin, and 2 μg/ml biopterin. The number of viable parasites in each ear was determined from the highest dilution at which promastigotes could be grown after a week of incubation at 26°C.

BMC and monocyte transfers. Mixture of BMCs was adjusted to 10^7 cells per ml in PBS and was incubated for 10 minutes at 37°C in 5 μM CFSE. After 2 washes in PBS supplemented with 10% heat-inactivated fetal bovine serum, 50×10^6 BMCs were resuspended in 300 μl PBS and injected intravenously in recipient mice. Monocytes were purified from the bone marrow of ubiquitin-GFP mice using a Monocyte Isolation Kit (Miltenyi Biotec).

In vitro cell culture and infection. Mice were sacrificed, and peritoneal macrophages were isolated by injecting 5 ml chilled PBS into the peritoneum and aspirating the cell suspension. Cells were put in culture in RPMI supplemented with 10% heat-inactivated fetal bovine serum and penicillin/streptavidin (Invitrogen Life Technologies). In Transwell experiments, inserts with a pore size of 0.4 μm (Merck Millipore) were used. For infection of the macrophages, stationary-phase DsRed-expressing promastigotes were incubated in RPMI supplemented with 4% mouse serum over 20 minutes. After washing, parasites were resuspended in RPMI supplemented with 0.7% BSA (Sigma-Aldrich) and penicillin/streptavidin and added to cell cultures. After 2 hours, macrophages were washed several times before being put back in culture medium. Two days later, iNOS was induced by adding IFN-γ (R&D Systems) and LPS (*E. coli* O26:B6, Sigma-Aldrich) to the medium at 10 ng/ml and 1 μg/ml, respectively. Flow cytometry analysis was performed 48 or 72 hours after induction. To measure concentrations of NO derivatives in activated macrophages, cells were incubated after surface staining for 30 minutes at 37°C with DAF-FM diacetate (Interchim) at 2 μM in PBS and analyzed by flow cytometry.

Flow cytometry. Ears were separated into dorsal and ventral sheets using jagged forceps and digested in RPMI 1640 medium containing 1 mg/ml collagenase and 50 ng/ml DNase (Sigma-Aldrich) for 45 minutes at 37°C and then passed through a 70-μm cell strainer. Cell suspensions were fixed for 1 hour at 4°C using a 2% methanol-free formaldehyde solution (Polysciences) in PBS. For iNOS and TNF-α staining, cells were permeabilized using Perm/Wash solution (BD Biosciences) according to the manufacturer's instructions and stained with goat anti-NOS2 polyclonal IgG (Santa Cruz Biotechnology) and DyLight-649–conjugated anti-goat secondary antibody (Jackson ImmunoResearch) or with APC-conjugated anti–TNF-α (clone MP6-XT22) antibody (BioLegend). Surface staining of cells was performed using APC-eFluor780–conjugated anti-CD45.2 (clone 104), PE-Cy7–conjugated anti-CD45.1 (clone A20), APC-eFluor780– or PerCP-Cy5.5–conjugated anti-CD11b (clone M1/70), eFluor660-conjugated anti-CD11c (clone N418), eFluor450-conjugated anti-I-A and I-E (clone M5/114.15.2), and PE-Cy7–conjugated anti-Gr-1 (clone RB6-8C5) antibodies (all from eBioscience); Pacific Blue–conjugated anti-CD45.2 (clone 104) antibody (BioLegend); APC-Cy7–conjugated anti-CD45 (clone 30F11) antibody (BD Biosciences); or APC-conjugated anti-CCR2 (clone 475301) antibody (R&D Systems). All cell preparations were F_c-blocked using anti-CD16/32 antibody (eBiosciences) prior to staining and analyzed on a FACSCanto cytometer (BD Biosciences). Data were analyzed using FlowJo software (TreeStar). To determine NO effect on extracellular *L. major* parasites were stained with APC-labeled Annexin V (BD Pharmingen) according to the manufacturer's instructions and analyzed using a LSRII flow cytometer in combination with FACSDiva software (BD Biosciences). Cell sorting was performed using a FACSAria II (BD Bioscience).

Intravital imaging. Mice were anesthetized and prepared for intravital microscopy as described previously (29). A coverslip surrounded by parafilm was placed onto the ear and covered with deionized water to immerge a 25×/1.05 NA objective (Olympus). Two-photon imaging was performed using a DM6000 upright microscope equipped with a SP5 confocal head (Leica Microsystems) and a Chameleon Ultra Ti:Sapphire laser (Coherent) tuned at 920 nm. Emitted fluorescence was passed to nondescanned detectors through dichroic mirrors. Typically, images from 20 to 25 z planes

spaced 2 μm were collected every 2 to 3 minutes for up to 5 hours. Intravital 3-dimensional time series were processed and superimposed using the Imaris software (Bitplane).

Time-lapse microscopy on cell cultures. Infected macrophages were activated as described previously. After 8 to 20 hours, phase-contrast and fluorescence images were recorded every 10 minutes at various positions for a total duration of 30 to 48 hours, using a DMI 6000B inverted microscope (Leica Microsystems) equipped with an environmental chamber for temperature, humidity, and CO2 (PECON), with a 20×/0.75 NA dry objective (Olympus) and a CoolSNAP HQ2 Roper camera (Photometrics). Macrophages remained alive and motile during the entire recording period. Parasite and cell tracking was performed with Imaris software (Bitplane).

Statistics. Unless otherwise indicated in the legends, data in graphs with errors bars represent mean ± SEM. Statistical analyzes on multiple groups were performed using a 1-way ANOVA, followed by a Tukey column pair comparison post-test in the Prism 5 software. Two-group data sets were analyzed using a Mann-Whitney test. A *P* value of less than 0.05 was considered as significant.

1. MacMicking JD. Interferon-inducible effector mechanisms in cell-autonomous immunity. *Nat Rev Immunol*. 2012;12(5):367–382.
2. Fang FC. Antimicrobial reactive oxygen and nitrogen species: concepts and controversies. *Nat Rev Microbiol*. 2004;2(10):820–832.
3. Kaye P, Scott P. Leishmaniasis: complexity at the host-pathogen interface. *Nat Rev Microbiol*. 2011; 9(8):604–615.
4. Liew FY, Millott S, Parkinson C, Palmer RM, Moncada S. Macrophage killing of Leishmania parasite in vivo is mediated by nitric oxide from L-arginine. *J Immunol*. 1990;144(12):4794–4797.
5. Wei XQ, et al. Altered immune responses in mice lacking inducible nitric oxide synthase. *Nature*. 1995; 375(6530):408–411.
6. Evans TG, Thai L, Granger DL, Hibbs JB, Hibbs JB Jr. Effect of in vivo inhibition of nitric oxide production in murine leishmaniasis. *J Immunol*. 1993; 151(2):907–915.
7. Stenger S, Donhauser N, Thuring H, Rollinghoff M, Bogdan C. Reactivation of latent leishmaniasis by inhibition of inducible nitric oxide synthase. *J Exp Med*. 1996;183(4):1501–1514.
8. Farlik M, et al. Nonconventional initiation complex assembly by STAT and NF-κB transcription factors regulates nitric oxide synthase expression. *Immunity*. 2010;33(1):25–34.
9. Liew FY, Li Y, Millott S. Tumor necrosis factor-alpha synergizes with IFN-γ in mediating killing of Leishmania major through the induction of nitric oxide. *J Immunol*. 1990;145(12):4306–4310.
10. Xie QW, Whisnant R, Nathan C. Promoter of the mouse gene encoding calcium-independent nitric oxide synthase confers inducibility by interferon gamma and bacterial lipopolysaccharide. *J Exp Med*. 1993;177(6):1779–1784.
11. Gao JJ, Zuvanich EG, Xue Q, Horn DL, Silverstein R, Morrison DC. Cutting edge: bacterial DNA and LPS act in synergy in inducing nitric oxide production in RAW 264.7 macrophages. *J Immunol*. 1999; 163(8):4095–4099.
12. Muhl H, Bachmann M, Pfeilschifter J. Inducible NO synthase and antibacterial host defence in times of Th17/Th22/T22 immunity. *Cell Microbiol*. 2011; 13(3):340–348.
13. Pautz A, Art J, Hahn S, Nowag S, Voss C, Kleinert H. Regulation of the expression of inducible nitric oxide synthase. *Nitric Oxide*. 2010;23(2):75–93.
14. Tian L, Noelle RJ, Lawrence DA. Activated T cells enhance nitric oxide production by murine splenic macrophages through gp39 and LFA-1. *Eur J Immunol*. 1995;25(1):306–309.
15. Lima-Junior DS, et al. Inflammasome-derived IL-1beta production induces nitric oxide-mediated resistance to Leishmania. *Nature Med*. 2013; 19(7):909–915.
16. Wakil AE, Wang ZE, Ryan JC, Fowell DJ, Locksley RM. Interferon gamma derived from CD4(+) T cells is sufficient to mediate T helper cell type 1 development. *J Exp Med*. 1998;188(9):1651–1656.
17. Mougneau E, Bihl F, Glaichenhaus N. Cell biology and immunology of Leishmania. *Immunol Rev*. 2011; 240(1):286–296.
18. Sacks D, Noben-Trauth N. The immunology of susceptibility and resistance to Leishmania major in mice. *Nat Rev Immunol*. 2002;2(11):845–858.
19. Bogdan C, Rollinghoff M, Diefenbach A. Reactive oxygen and reactive nitrogen intermediates in innate and specific immunity. *Curr Opin Immunol*. 2000;12(1):64–76.
20. Bogdan C. Nitric oxide and the immune response. *Nat Immunol*. 2001;2(10):907–916.
21. Chakravortty D, Hansen-Wester I, Hensel M. Salmonella pathogenicity island 2 mediates protection of intracellular Salmonella from reactive nitrogen intermediates. *J Exp Med*. 2002;195(9):1155–1166.
22. Davis AS, Vergne I, Master SS, Kyei GB, Chua J, Deretic V. Mechanism of inducible nitric oxide synthase exclusion from mycobacterial phagosomes. *PLoS Pathog*. 2007;3(12):e186.
23. Flannagan RS, Cosio G, Grinstein S. Antimicrobial mechanisms of phagocytes and bacterial evasion strategies. *Nat Rev Microbiol*. 2009;7(5):355–366.
24. Bogdan C, Donhauser N, Doring R, Rollinghoff M, Diefenbach A, Rittig MG. Fibroblasts as host cells in latent leishmaniosis. *J Exp Med*. 2000; 191(12):2121–2130.
25. Misslitz A, Mottram JC, Overath P, Aebischer T. Targeted integration into a rRNA locus results in uniform and high level expression of transgenes in Leishmania amastigotes. *Mol Biochem Parasitol*. 2000; 107(2):251–261.
26. Sorensen M, Lippuner C, Kaiser T, Misslitz A, Aebischer T, Bumann D. Rapidly maturing red fluorescent protein variants with strongly enhanced brightness in bacteria. *FEBS Lett*. 2003;552(2–3):110–114.
27. De Trez C, Magez S, Akira S, Ryffel B, Carlier Y, Muraille E. iNOS-producing inflammatory dendritic cells constitute the major infected cell type during the chronic Leishmania major infection phase of C57BL/6 resistant mice. *PLoS Pathog*. 2009; 5(6):e1000494.
28. Peters NC, et al. In vivo imaging reveals an essential role for neutrophils in leishmaniasis transmitted by sand flies. *Science*. 2008;321(5891):970–974.
29. Filipe-Santos O, et al. A dynamic map of antigen recognition by CD4 T cells at the site of Leishmania major infection. *Cell Host Microbe*. 2009;6(1):23–33.
30. Serbina NV, Jia T, Hohl TM, Pamer EG. Monocyte-mediated defense against microbial pathogens. *Annu Rev Immunol*. 2008;26:421–452.
31. Serbina NV, Shi C, Pamer EG. Monocyte-mediated immune defense against murine Listeria monocytogenes infection. *Adv Immunol*. 2012;113:119–134.
32. Leon B, Lopez-Bravo M, Ardavin C. Monocyte-derived dendritic cells formed at the infection site control the induction of protective T helper 1 responses against Leishmania. *Immunity*. 2007; 26(4):519–531.
33. Müller AJ, Filipe-Santos O, Eberl G, Aebischer T, Späth GF, Bousso P. CD4+ T cells rely on bystander effector activity to control local infection. *Immunity*. 2012;37(1):147–157.
34. de Veer MJ, et al. MyD88 is essential for clearance of Leishmania major: possible role for lipophosphoglycan and Toll-like receptor 2 signaling. *Eur J Immunol*. 2003;33(10):2822–2831.
35. Fonseca SG, et al. TNF-α mediates the induction of nitric oxide synthase in macrophages but not in neutrophils in experimental cutaneous leishmaniasis. *Eur J Immunol*. 2003;33(8):2297–2306.
36. Fromm PD, Kling J, Mack M, Sedgwick JD, Korner H. Loss of TNF signaling facilitates the development of a novel Ly-6C(low) macrophage population permissive for Leishmania major infection. *J Immunol*. 2012;188(12):6258–6266.
37. Sarkar A, et al. Monitoring of intracellular nitric oxide in leishmaniasis: its applicability in patients with visceral leishmaniasis. *Cytometry A*. 2011;79(1):35–45.
38. Mauel J, Ransijn A. Leishmania spp.: mechanisms of toxicity of nitrogen oxidation products. *Exp Parasitol*. 1997;87(2):98–111.
39. Gao JJ, Filla MB, Fultz MJ, Vogel SN, Russell SW, Murphy WJ. Autocrine/paracrine IFN-αβ mediates the lipopolysaccharide-induced activation of transcription factor Stat1α in mouse macrophages: pivotal role of Stat1α in induction of the inducible nitric oxide synthase gene. *J Immunol*. 1998; 161(9):4803–4810.
40. Swihart K, et al. Mice from a genetically resistant background lacking the interferon gamma receptor are susceptible to infection with Leishmania major but mount a polarized T helper cell 1-type CD4+ T cell response. *J Exp Med*. 1995;181(3):961–971.
41. Wang ZE, Reiner SL, Zheng S, Dalton DK, Locksley RM. CD4+ effector cells default to the Th2 pathway in interferon γ-deficient mice infected with Leishmania major. *J Exp Med*. 1994;179(4):1367–1371.
42. Abou Fakher FH, Rachinel N, Klimczak M, Louis J, Doyen N. TLR9-dependent activation of dendritic cells by DNA from Leishmania major favors Th1

cell development and the resolution of lesions. *J Immunol.* 2009;182(3):1386–1396.

43. Naik S, et al. Compartmentalized control of skin immunity by resident commensals. *Science.* 2012; 337(6098):1115–1119.

44. Moll H, Binoder K, Bogdan C, Solbach W, Rollinghoff M. Production of tumour necrosis factor during murine cutaneous leishmaniasis. *Parasite Immunol.* 1990;12(5):483–494.

45. Darrah PA, et al. Multifunctional TH1 cells define a correlate of vaccine-mediated protection against Leishmania major. *Nat Med.* 2007;13(7):843–850.

46. Lukacs-Kornek V, et al. Regulated release of nitric oxide by nonhematopoietic stroma controls expansion of the activated T cell pool in lymph nodes. *Nat Immunol.* 2011;12(11):1096–1104.

47. Hibbs JB, Hibbs JB Jr, Taintor RR, Vavrin Z. Macrophage cytotoxicity: role for L-arginine deiminase and imino nitrogen oxidation to nitrite. *Science.* 1987;235(4787):473–476.

48. Karupiah G, Xie QW, Buller RM, Nathan C, Duarte C, MacMicking JD. Inhibition of viral replication by interferon-γ-induced nitric oxide synthase. *Sci-*

ence. 1993;261(5127):1445–1448.

49. Linares E, Giorgio S, Mortara RA, Santos CX, Yamada AT, Augusto O. Role of peroxynitrite in macrophage microbicidal mechanisms in vivo revealed by protein nitration and hydroxylation. *Free Radic Biol Med.* 2001;30(11):1234–1242.

50. Proudfoot L, et al. Regulation of the expression of nitric oxide synthase and leishmanicidal activity by glycoconjugates of Leishmania lipophosphoglycan in murine macrophages. *Proc Natl Acad Sci U S A.* 1996;93(20):10984–10989.

51. Wilkins-Rodriguez AA, Escalona-Montano AR, Aguirre-Garcia M, Becker I, Gutierrez-Kobeh L. Regulation of the expression of nitric oxide synthase by Leishmania mexicana amastigotes in murine dendritic cells. *Exp Parasitol.* 2010;126(3):426–434.

52. Müller AJ, Aeschlimann S, Olekhnovitch R, Dacher M, Späth GF, Bousso P. Photoconvertible pathogen labeling reveals nitric oxide control of Leishmania major infection in vivo via dampening of parasite metabolism. *Cell Host Microbe.* 2013;14(4):460–467.

53. Madsen L, et al. Mice lacking all conventional MHC class II genes. *Proc Natl Acad Sci U S A.* 1999;

96(18):10338–10343.

54. Huang S, et al. Immune response in mice that lack the interferon-gamma receptor. *Science.* 1993; 259(5102):1742–1745.

55. Schaefer BC, Schaefer ML, Kappler JW, Marrack P, Kedl RM. Observation of antigen-dependent CD8+ T-cell/ dendritic cell interactions in vivo. *Cell Immunol.* 2001;214(2):110–122.

56. Kawai T, Adachi O, Ogawa T, Takeda K, Akira S. Unresponsiveness of MyD88-deficient mice to endotoxin. *Immunity.* 1999;11(1):115–122.

57. Rothe J, et al. Mice lacking the tumour necrosis factor receptor 1 are resistant to TNF-mediated toxicity but highly susceptible to infection by Listeria monocytogenes. *Nature.* 1993;364(6440):798–802.

58. Laubach VE, Shesely EG, Smithies O, Sherman PA. Mice lacking inducible nitric oxide synthase are not resistant to lipopolysaccharide-induced death. *Proc Natl Acad Sci U S A.* 1995;92(23):10688–10692.

59. Efron DT, Most D, Shi HP, Tantry US, Barbul A. Modulation of growth factor and cytokine expression by nitric oxide during rat colon anastomotic healing. *J Gastrointest Surg.* 2003;7(3):393–399.